Theoretical study of GaN growth: A Monte Carlo approach

Kung Wang, Jasprit Singh, and Dimitris Pavlidis
Department of Electrical Engineering and Computer Science, The University of Michigan, Ann Arbor, Michigan 48109-2122

(Received 22 November 1993; accepted for publication 3 June 1994)

An atomistic model consistent with a variety of experimental observations is developed for GaN growth by molecular-beam epitaxy. The model is used in Monte Carlo simulation to study the impact of substrate temperature, Ga flux, and V/III (group-V element to group-III element) ratio on growth rate and growth front quality. The growth rate increases with the V/III ratio reaching a saturation value which is determined by the Ga flux. The quality of the growth front improves by using a smaller Ga flux for a fixed temperature and V/III ratio or by reducing the V/III ratio at a given temperature. A consideration of the growth kinetics suggests that GaN grown surfaces are likely to be Ga stabilized. These theoretically estimated trends are evidenced by two-dimensional and three-dimensional growth front contours evaluated under various growth conditions.

I. INTRODUCTION

Gallium nitride (GaN) is one of the most promising wide-band-gap semiconductors for applications in optoelectronic devices in the blue and ultraviolet (UV) wavelengths, and in high-temperature and high-power electronic devices.[1] In the past several years, a number of notable advances have been reported in the growth of GaN;[2–5] however, the success of GaN-based electronic and optoelectronic devices has been limited due to the presence of large unintended donor concentrations, the lack of high-quality lattice-matched substrates, and the difficulty in controlling electronic properties. High n-type background carrier concentration is believed to be resulting from native defects commonly thought to be nitrogen vacancies.[6] The challenge of the growth of high-quality GaN can be appreciated by noting the following observations.

(i) The vapor pressure of N_2 on GaN at 800 °C is close to 1 atm and becomes about 1000 atm at 1200 °C.[7] This poses a serious problem in incorporation of N into GaN at high growth temperatures.

(ii) Molecular nitrogen does not chemisorb on GaN due to the strong N—N bond in the N_2 molecule.[8] Thus atomic N has to be provided or other nitrogen-containing molecules such as NH_3 have to be used. In contrast in the growth of GaAs, As_2 is a perfectly suitable molecule for high-quality growth.

The above observations suggest that there are serious contradictory forces at play in the growth of GaN since one needs low growth temperature to suppress N reevaporation and film decomposition during growth, while at the same time a sufficiently high temperature is necessary for dissociative chemisorption of N from its molecular form. Additionally, the growth kinetics involving the surface migration of Ga and N after incorporation may place further restrictions on the growth conditions.

Little is known about the growth mechanisms of this "new" member of the III-V family. This article is motivated by a desire to understand how certain growth conditions control incorporation of nitrogen and eventually to understand the growth mechanism of GaN.

The thermodynamics, kinetics, and the microscopic details of incorporation of atoms play very important roles in controlling the quality of growth.[9] To fully understand these important issues, an atomistic understanding of GaN growth must be developed. In this article, a model for nitrogen incorporation in molecular-beam-epitaxy-like (MBE-like) growth of GaN is presented. A theoretical study based on Monte Carlo techniques is carried out. The importance of group-V element to group-III element (V/III) flux ratios, growth temperatures, and Ga flux on the growth quality of GaN are examined. The results obtained appear to be consistent with experimental electron-cyclotron-resonance microwave-plasma-assisted MBE (ECR-MBE) growth data of GaN.[10]

II. THEORETICAL MODEL

A. Monte Carlo approach and application of GaN growth modeling

A first attempt in simulating the growth of GaN can be made by considering MBE-like conditions. This provides very useful information regarding the growth mechanisms by avoiding at the same time the complexity arising by chemical reactions as, for example, in metal-organic chemical-vapor desorption (MOCVD).

Since molecular nitrogen does not react with gallium under normal MBE-growth conditions, providing atomic nitrogen has been a major issue for this technique. Three approaches have been explored to grow GaN by MBE-like conditions, namely, gas-source MBE (GSMBE),[11] ECR-MBE,[10] and reactive-ion MBE (RIMBE).[8]

ECR-MBE-like conditions were chosen for our simulations at this stage because of the relatively simple processes involved in this case. In ECR MBE, the ECR source is used to produce the atomic nitrogen and gallium comes from the conventional Knudsen effusion cell. Typical growth conditions[10] are: Ga fluxes of 3.7×10^{14} $cm^{-2}\,s^{-1}$; substrate temperatures of 400–750 °C; and nitrogen partial pressure of $\sim10^{-4}$ Torr. The growth rate is about 2.5 μm/min and best crystallinity was achieved around 600 °C.

 0021-8979/94/76(6)/3502/9/$6.00 © 1994 American Institute of Physics

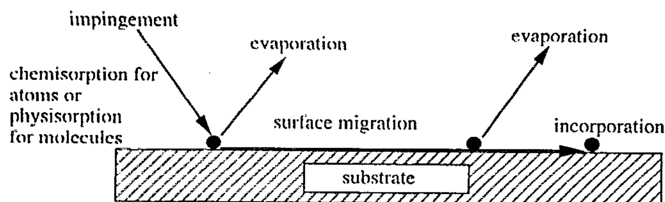

FIG. 1. Conceptual picture of MBE-like growth process.

GaN can form crystalline in two phases, namely, wurtzite (α-GaN) and zinc blende (β-GaN). Theoretical calculations predict that the total energies of the GaN wurtzite and zinc-blende phases are nearly equal.[12] The phase formation preference appears to be determined by the nucleation. Thus, the substrate on which GaN is grown has very strong influence on the crystal structure of GaN. The symmetry and the orientation of substrate materials provide a template for the nucleation of the crystal growth. GaN grown on hexagonal substrates has been of wurtzite structure[2] while GaN has been grown on cubic substrates of zinc-blende structure. Cubic GaN has been grown on (111) GaAs, (100) GaAs,[13] cubic SiC,[14] MgO,[15] and (001) Si.[16] Due to its higher symmetry, β-GaN is expected to have decreased photon scattering and higher ballistic electron velocities.[5] Also, β-GaN on GaAs is important due to its potential for devices integrated with other III-V materials. (001) GaAs has therefore been selected as the substrate for the simulation of the growth reported here. The calculated trends are, however, of more general nature and may be employed as general guidelines for understanding GaN growth.

The lattice gas model using Monte Carlo techniques has been quite successful in understanding the atomistic nature of the growth of III-V semiconductors,[9] such as GaAs, AlAs, and InAs, and II-VI systems as in HgTe-CdTe.[17] With some important modifications discussed below, we follow this formalism for the GaN system.

The dynamics of crystal growth from the vapor could be simulated by four basic events: impingement, surface reaction, surface migration, and evaporation. The modulated-beam studies of MBE-grown GaAs by Arthur[18] and by Foxon and Joyce[19] have shown that the impinging atomic Ga is directly adsorbed into a chemisorbed state, binding either with the As or Ga atoms on the surface. By contrast, the impinging As_2 or As_4 molecules are physisorbed into a weakly bonded state and retain their molecular nature. We apply these findings, of atomic species being chemisorbed while molecular species being physisorbed on the surface, to the MBE growth of GaN. In Fig. 1, we show a conceptual picture of the MBE-growth process for GaN. The first important ingredient in the growth is the incorporation of cations. The process of an atom impinging on a vacant site and forming chemical bonds will be called the chemisorption process. During the growth of GaN, the impinging atomic cation is directly absorbed into a chemisorbed state, binding with the anion atoms on the surface. Depending on growth conditions, chemisorbed atoms can then either evaporate or migrate at the surface. Following such a process there are again two possibilities for either atom incorporation or evaporation.

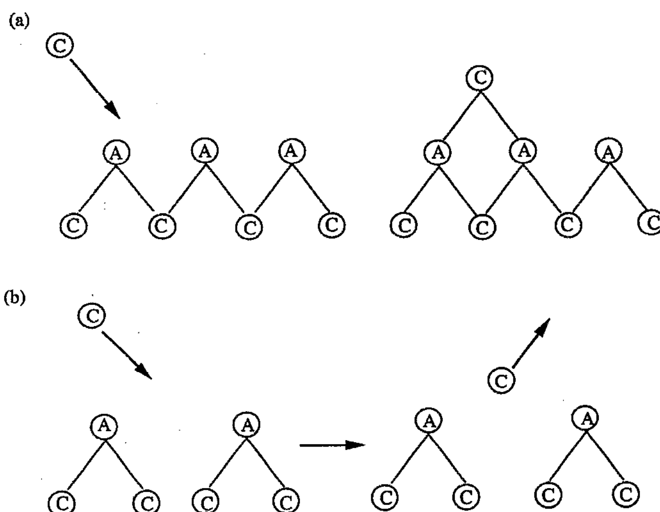

FIG. 2. (a) Atomic arrangement necessary for incorporation of a cation C; (b) atomic arrangement for which the impinging cation cannot be incorporated.

The need for, and significant consequences of, the property geometry for incorporation of cations can be readily appreciated by examining the (100) planes of a crystal. The alternating (100) planes are made up of cations or anions only, with atoms in a given plane forming two bonds with the atoms in the plane below and two bonds with the atoms in the plane above. Consequently, it is assumed that a cation can be incorporated into the structure only if it can form two bonds with the anion layer below. For this to occur, the anions have to be arranged in a specific manner. In Fig. 2(a) a cation (C) impinging at the site shown is incorporated into the growing structure, while a cation impinging on the site shown in Fig. 2(b) cannot be incorporated since the two anions (A) necessary for bonding are not available.

The incorporation process of atomic N is assumed to be similar to that of Ga; however, since the vapor pressure of N is much higher than that of Ga in the normal growth temperatures, one can expect that the incorporation of nitrogen would be more difficult. Due to the volatile property of nitrogen, even though impinging nitrogen is chemisorbed, it still has a very high probability to move around. Once it meets another nitrogen atom, they will form a molecule and evaporate immediately. To ensure incorporation, more bonds have to be formed to trap nitrogen. We discuss more details about nitrogen incorporation after examining the evaporation rates of the elements involved in this process.

After the atoms are chemisorbed in the growing structure, internal energy and the surface kinetic rates for migration and evaporation determine the nature of growth. The following Hamiltonian is used to describe the energetics of the system:

$$H=\frac{1}{2}\left(\sum_{iaic} C_{ia}V_{AC}C_{ic}+\sum_{iaia} C_{ia}V_{AA}C_{ia}+\sum_{icic} C_{ic}V_{CC}C_{ic}\right), \quad (1)$$

where ia and ic denote the anion or the cation at the site i; C_{ia} nd C_{ic} denotes the occupations of the sites ia and ic, respectively, and V_{AC}, V_{AA}, and V_{CC} are the bond energies for the nearest-neighbor, second-nearest-neighbor anion, and second-neighbor cation bonds, respectively.

The kinetic processes are described by the evaporation and diffusion rates. The evaporation rate R_e^i is taken to be of an Arrhenius form,

$$R_e^i = R_{0e}^i \exp(-E_{\text{evap}}^i / K_B T), \tag{2}$$

where i is the site for the cation or anion under question; R_{0e} is a prefactor for evaporation and E_{evap}^i is the activation energy of the atom in the site i.

Migration rates are taken to be in an Arrhenius form as well,

$$R_d^i = R_{0d}^i \exp[-(E_{\text{tot}}^i - \Delta)/k_B T], \tag{3}$$

where R_{0d} is a prefactor; E_{tot}^i is the total energy at site i; Δ is a parameter that is related to the energy adjustment for a particular migration process, and $(E_{\text{tot}}^i - \Delta)$is the activation barrier for migrations. Since nitrogen atoms have very high probability of migration, the limiting kinetics controlling the growth are the cation (gallium) surface kinetics; a more detailed discussion about this follows later on in Sec. II B. Migration rates were therefore considered only for Ga. Four migration processes were considered: (a) hopping on the same surface layer in a direction which is defined by the intercept of the surface and orbital planes; (b) hopping on the same surface layer in a direction which is perpendicular to the intercept line of the surface and orbital planes; (c) hopping to the lower layer; (d) hopping to the upper layer. The energy barrier for hopping to occur by mechanism (a) is equal to breaking half of its bonds with the atoms in the layers below it. The energy barriers for other hopping are equal to breaking 3/4 bonds. Figure 3 shows interlayer and interlayer hopping, where $E_\parallel$ and $E_\perp$ are the energy adjustment for the intralayer and interlayer hopping, respectively.

The bond energies necessary for the above energy barrier evaluation can be estimated using the activation energy barrier estimated from vapor pressure versus $1/T$ data of Ga over GaN. Since the vapor pressure data of Ga over GaN are not available, scaling based on the ratio of the atomization energies of GaN and GaAs is used to approximate the bond energies of Ga-N and Ga-Ga.

For GaAs,[20] the bond energy values are

$$V_{\text{Ga-As}} = 0.8 \text{ eV}, \quad V_{\text{Ga-Ga}} = 0.17 \text{ eV}. \tag{4}$$

The atomization energy values[21] are: ~157.8 kpm (kilocalorie per mole) and ~200.9 kpm for GaAs and GaN, respectively. The scaled bond energies, V_{AC} and V_{CC}, for GaN can consequently be approximated to be

$$V_{\text{Ga-N}} = 1.02 \text{ eV}, \quad V_{\text{Ga-Ga}} = 0.22 \text{ eV}. \tag{5}$$

The gallium evaporation energy E_{evap} of Eq. (2) is assumed to be equal to the total bond energy of a kink site E_{tot}. The kink site is defined as a site at a step edge where an atom has two nearest- and six second-nearest-neighbor bonds established,

$$E_{\text{evap}} = E_{\text{tot}} = 2V_{\text{Ga-N}} + 6V_{\text{Ga-Ga}}. \tag{6}$$

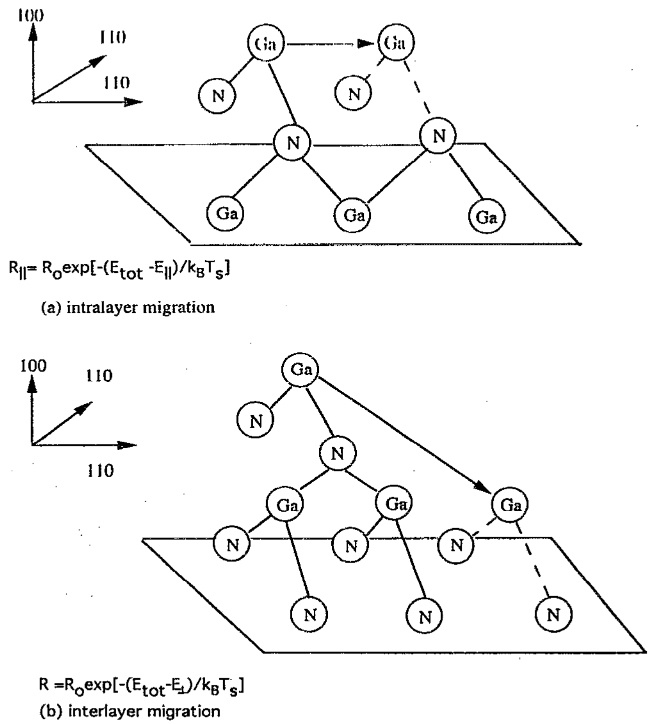

FIG. 3. (a) Hopping in the same layer ($E_\parallel$ is the activation barrier). (b) Hopping to the lower layer ($E_\perp$ is the activation barrier). k_B is the Boltzman constant.

The prefactor $R_{0e}^{\text{Ga}}$of Eq. (2) is approximated to be equal to that of GaAs, namely, $R_{0e}^{\text{Ga}} = 8 \times 10^{13} \text{ s}^{-1}$ for Ga atoms.[20]

The evaluation rate $R_e^N$for the nitrogen anion was determined using the vapor pressure versus temperature data by Karpinski.[22] This can be expressed as follows:

$$R_e^{\text{N}} = 1.35 \times 10^{22} \exp(-3.17/k_B T). \tag{7}$$

The bond energy V_{AA} between second-neighbor nitrogen atoms is chosen to be $V_{\text{N-N}} = 0.18$ eV. The prefactor R_{0d} of hopping is controlled by the phonon frequency and represents the attempt frequency for the hop. It is known that for atoms the value of R_{0d} can vary anywhere from 10^5 to 10^{11} s^{-1}. There have been a few attempts to measure R_{0d} for Ga atoms on GaAs using a masked growth technique[23] and reflection high-energy electron diffraction (RHEED) studies.[24] These suggested that Ga atoms can move over about 2000 Å in the absence of As overpressure. Furthermore, vapor pressure studies of GaN show nitrogen evaporation in molecular form and a much higher vapor pressure of nitrogen over GaN than for Ga over GaN. As a result, a higher surface migration rate can be expected for the nitrogen atoms compared with Ga. Based on the above information and the results of GaAs growth simulations, the values of $3.5 \times 10^{10} \text{ s}^{-1}$ and 3×10^{11} s^{-1} were chosen for Ga and N, respectively, in this simulation. Tables I and II show our estimated migration (hops/s) and evaporation rates (atoms/s) for Ga and evaporation rates (atoms/s) for N atoms on the surface at different substrate temperature. In these tables the argument (m,n) represents a configuration with m nearest neighbors and n second-nearest neighbors.

TABLE I. Rates of migration $R_d(m,n)$ (hops/s) and evaporation $R_e(m,n)$ (atoms/s) for Ga on the (100) surface as a function of substrate temperature.

T (°C)	$R_e(2,4)$ $R_d(2,4)$	$R_e(2,5)$ $R_d(2,5)$	$R_e(2,6)$ $R_d(2,6)$	$R_e(2,7)$ $R_d(2,7)$
400	9×10^{-9} 0.38	2.2×10^{-10} 5.6×10^{-2}	4.9×10^{-12} 8.4×10^{-3}	1.1×10^{-13} 1.3×10^{-3}
500	6.7×10^{-6} 9.9	2.5×10^{-7} 1.9	8×10^{-9} 0.36	3.3×10^{-10} 6.9×10^{-2}
600	1.02×10^{-3} 1.22×10^{2}	5.5×10^{-5} 28.2	2.9×10^{-6} 6.5	1.6×10^{-7} 1.5
700	5.6×10^{-2} 9×10^{2}	4×10^{-3} 2.4×10^{2}	2.9×10^{-4} 64.9	2.1×10^{-5} 17.4
800	1.5 4.6×10^{3}	0.13 1.4×10^{3}	1.2×10^{-2} 421.5	1.1×10^{-3} 127.9

In conventional Monte Carlo methods,[9] the kinetic processes of the growth are treated as individual random events. A probability distribution function is established to describe the probability of each event happening. A random number is then generated to compare with the distribution function, and to decide which event happens. The kinetic rates developed previously are used to construct the probability distribution function. As one can see from Table II, the nitrogen evaporation rates become extremely large at high temperatures. For example, at the usually employed ECR-MBE-growth temperature for GaN of ~600 °C, the evaporation rates of nitrogen are four order of magnitude higher than the maximum values of the other major kinetic processes such as Ga migration and evaporation. This feature not only causes experimental difficulties, but also creates a special problem in computer simulation. Due to the high evaporation and migration rates of nitrogen, it is required to study more than 10^{12} events to simulate the growth of 10 monolayers of GaN for a 30×30 site area if conventional Monte Carlo approaches are used. This makes it prohibitively long for practical simulations. Also this indicates the growth mechanism of GaN may be different from that of the conventional III-V materials such as GaAs. The new model has to be developed for the simulation of GaN.

B. Specific modeling issues related to GaN growth

As one can see from Tables I and II, there is a large difference between the evaporation rates for Ga and N at similar temperatures. Since the nitrogen evaporation rate is extremely high particularly at the high temperature usually

TABLE II. Rates of nitrogen evaporation $R_e(m,n)$ (atoms/s) on the (100) surface as a function of substrate temperature.

T (° C)	$R_e(2,4)$	$R_e(2,5)$	$R_e(2,6)$	$R_e(2,7)$
400	31.4	1.2	4.4×10^{-2}	1.7×10^{-3}
500	1.6×10^{4}	919	52.7	3.02
600	2.0×10^{6}	1.6×10^{5}	1.2×10^{4}	990
700	8.9×10^{7}	9.2×10^{6}	9.5×10^{5}	9.8×10^{4}
800	2.0×10^{9}	2.6×10^{8}	3.3×10^{7}	4.2×10^{6}

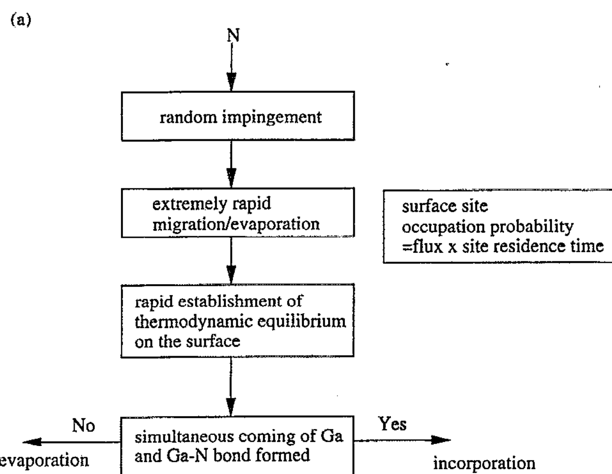

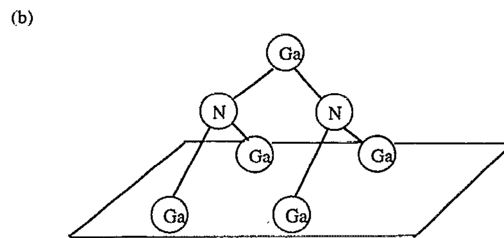

FIG. 4. (a) A conceptual picture of the N incorporation process. (b) Nitrogen atoms "trapped" by gallium atoms.

required for growth, the residence time of a nitrogen atom is then much smaller than that of Ga. Furthermore, experimental evidence from growth of GaN indicates that the sticking coefficient of Ga is small (0.25) but not zero, and any attempt to increase the Ga flux leads to a Ga-rich film.[25] An important point that emerges from these results is that the growing surface of GaN may very likely be cation stabilized. This would then result in nonstoichiometric GaN film which could account for the often observed high unintended carrier concentrations. Furthermore, the incorporation of Ga appears to be limited by the supply of nitrogen radicals at the growth surface. It could consequently be expected that the incorporation of Ga and N are related. Accordingly, a tentative model for N incorporation could be drawn and is discussed below.

1. N and Ga incorporation model

A conceptual picture of N incorporation is shown in Fig. 4. When the nitrogen atom impinges, it could reach thermodynamic equilibrium with the surface in a short tine. During the residence time of the absorbed nitrogen atom, only if at the same time a Ga atom comes to its top, and forms a bond which "traps" the nitrogen atom, would the nitrogen atom be incorporated; otherwise the nitrogen atom would reevaporate very rapidly. As a result, a tetrahedral binding structure would be formed in the [100] direction, where each Ga traps two nitrogen atoms. Another possibility would of course be N incorporation by the formation of surface N—N bonds. These are, however, much weaker than the Ga—N bonds and

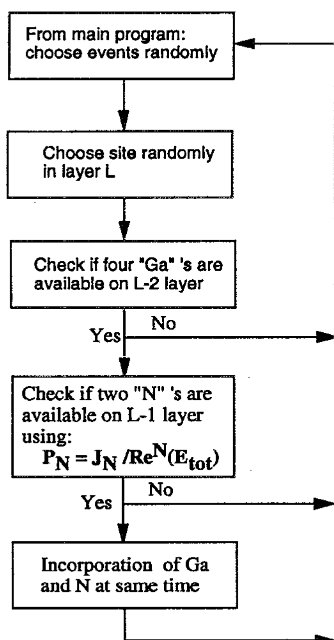

FIG. 5. A simplified flowchart for the special Monte Carlo approach used for Ga and N incorporation.

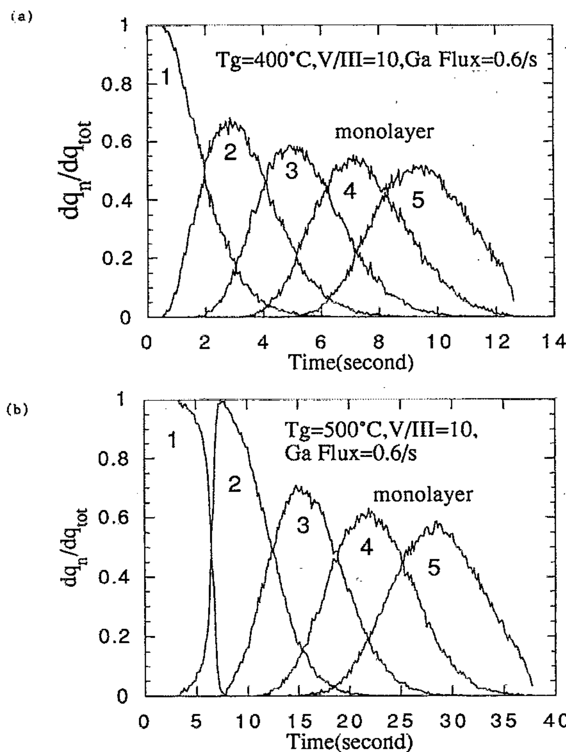

FIG. 7. (a) Ratio of nth layer coverage over total coverage vs growth temperature (T=400 °C, V/III=10, Ga flux=0.61/s); (b) ratio of nth layer coverage over total coverage vs growth temperature (T=500 °C, V/III=10, Ga flux=0.61/s).

it is therefore the latter that are favored. Overall we can consequently visualize this as a process where Ga keeps the N down on the surface.

Let us next examine the incorporation probability of nitrogen since it is crucial for increasing the efficiency of GaN growth simulation. The residence time of impinging nitrogen atoms is reversely proportional to the evaporation rate. The higher the evaporation rate, the shorter the residence time, and the smaller the probability that a nitrogen atom would be trapped. In addition, the more nitrogen atoms impinge, the higher are the chances for the nitrogen atoms to meet gallium atoms, and consequently the probability that they could be trapped by gallium atoms increases. The incorporation of nitrogen can consequently be described by a surface site occupation probability function $P_N(E_{tot})$. It will depend on both the site residence time and the available flux. For each of the growing sites i, this is defined through thermodynamics by

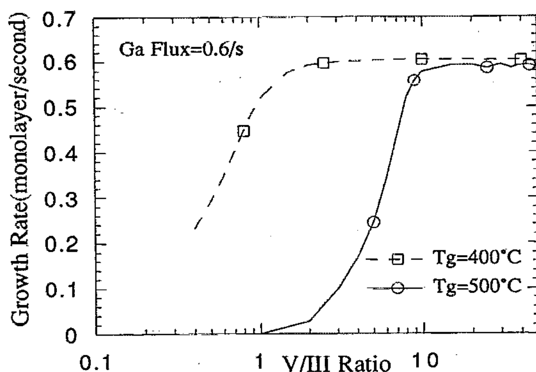

FIG. 6. Growth rate vs V/III ratio (Ga flux=0.6/s).

$$P_N(E_{tot}) = J_N / R_e(E_{tot}), \tag{8}$$

where J_N is the nitrogen flux and $R_e(E_{tot})$ is the evaporation rate for the site with energy E_{tot}. For the site under question for which the probability of N incorporation is evaluated, a random number is then generated. This is then used to describe whether the N atom is incorporated during the chemisorption of a Ga atom; N was considered to be incorporated only if P_N was larger than the random generated number.

Ga incorporation depends on the availability of two nitrogen atoms on the surface. The formation of two bonds between the Ga and the two N atoms ensures Ga incorporation. Thus incorporation is limited by the supply of nitrogen radicals at the grown surface. The nitrogen incorporation probability function was thus used to evaluate the Ga incorporation.

The above probability function was also used to evaluate Ga migration. Since Ga forms two bonds with the N atoms of the layer below it, migration of Ga requires that two such bonds are available at the site which it will move to. To estimate this availability we employed the probability function of Eq. (8).

From Eq. (8), $P_N(E_{tot})$ is inversely proportional to the evaporation rate $R_e(E_{tot})$ for given J_N. As we can see in Eq. (1), E_{tot} depends on the local environment, that is, the number of bonds that nitrogen can form. The more bonds the nitrogen can form, the larger the incorporation probability is for nitrogen. Table II shows clearly that N atoms have a high probability of being incorporated at sites where they have

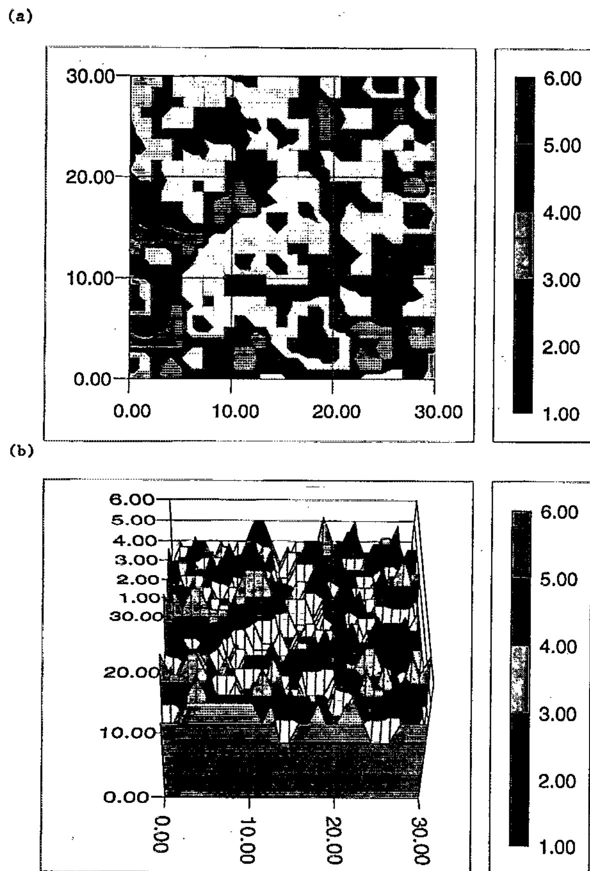

FIG. 8. (a) Growth front contour (T=400 °C, V/III=10); the legend on the right-hand side is the number of surface monolayers; (b) 3D plot of growth front (T=400 °C, V/III=10); the legend on the right-hand side is the number of surface monolayers.

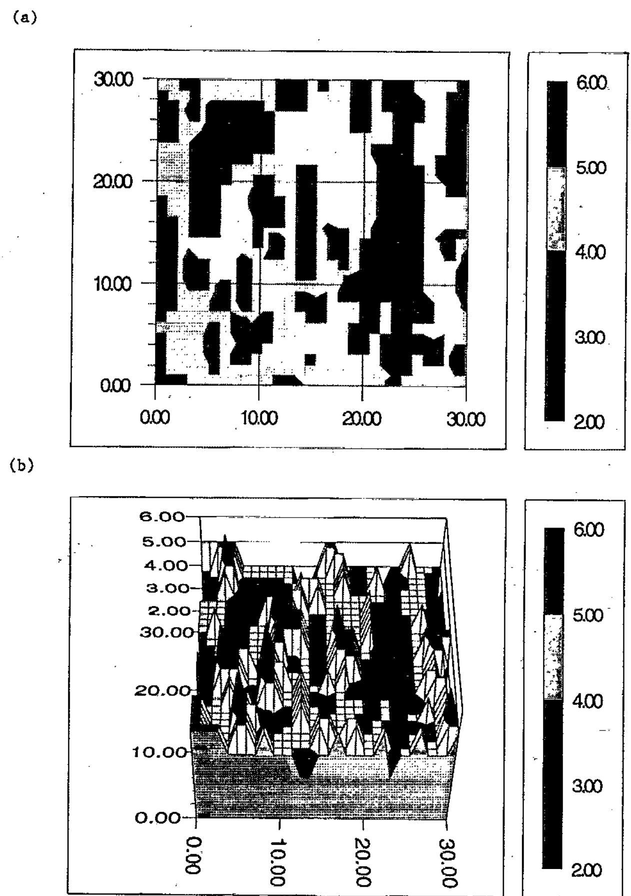

FIG. 9. (a) Growth front contour (T=500 °C, V/III=10); the legend on the right-hand side is the number of surface monolayers; (b) 3D plot of growth front (T=500 °C; V/III=10); the legend on the right-hand side is the number of surface monolayers.

strong bonding, e.g., the (2,6) or (2,7) kink-type surface site for the (100) growth. The bonding nature of the growing surface depends very much on the surface quality in terms of smoothness. As can be imagined physically, a smooth surface will primarily have exposed sites with very low energy, i.e., (2,4) site types. On the other hand, a rough surface is expected to have a large concentration of kink-type surface sites [i.e., (2,6) site types]. The implication of these results is that sample misorientation and surface preparation (polishing, chemical etching, thermal heating, buffer layer growth) play major roles in the incorporation of N atoms during nucleation and growth of GaN.

2. Surface stabilization and antisite defects

Since the sticking coefficients of Ga over Ga, Ga over N, N over Ga, and N over N are unknown for the GaN system, we can only speculate their values by considering experimental results available for GaAs. In particular one can consider that the sticking coefficient of Ga over N and N over Ga are unity and that the sticking coefficient of Ga over Ga is not zero. The N over N sticking coefficient was also considered different than zero since one normally deals in GaN growth with atomic N; unlike molecular N, i.e., N_2, atomic N reacts easily and the sticking coefficient can be thought to be different than zero. This contrasts GaAs growth where the As over As sticking coefficient is zero due to the presence of molecular As_2. Since the growing surface of GaN is likely to be cation stabilized and Ga-to-Ga bonds can be present, the GaN films could be nonstoichiometric with antisite defects. The latter could also account for the often observed high unintentional carrier concentrations. Antisite defects may also originate by another reason, namely a nonzero N-to-N sticking coefficient. In such a case GaN growth will differ considerably from traditional III-V growth. In the case of GaAs growth, As_2 over As has, for example, a sticking coefficient of zero. The zero sticking coefficient of As_2 permits consequently high V/III ratios without the risk of antisite defect creation which seems to occur in GaN.

Based on the above considerations, a special Monte Carlo simulation was carried out. A simplified flowchart is shown in Fig. 5. A 30×30 site area with periodic condition is chosen for the simulation and the results obtained are discussed in the following section. Sun workstations were used for the simulation. The computing time depends on the substrate temperature chosen for the simulation.

III. RESULTS OF GROWTH SIMULATION AND DISCUSSION

A. Impact of N/Ga flux ratio on the growth rate

First, the relation between the growth rate and V/III ratio, as well as the substrate temperature, was evaluated. From Fig. 6 one can see that the growth rate increases with the V/III ratio, reaching a saturation value which is determined by the Ga flux and is independent of temperature. The V/III ratio at which this saturation value is reached is determined by the substrate temperature. Furthermore, since the growth rate is determined by the Ga flux (see Sec. III D, Fig. 13), an increase of V/III ratio is accompanied by an enhancement in the Ga incorporation. Figure 6 also shows that a critical V/III ratio is required at each growth temperature for the growth rate to become significant.

B. Impact of the substrate temperature on the growth front

Figures 7(a) and 7(b), show the plots of [nth layer coverage (dq_n)]/[total coverage (dq_{tot})] as a function of growth time for constant Ga flux of 0.616/s. Here, q_n is the number of atoms contained in the nth layer. Similarly, q_{tot} is the number of atoms contained in all the grown layers; this refers to all layers completed and uncompleted from the point of view of growth. Thus, dq_n/dq_{tot} represents the ratio of the additional incorporated atoms in the nth layer with respect to the total incorporated atoms within a time interval dt. The significance of the dq_n/dq_{tot} ratio is in fact very similar to that obtained from RHEED oscillations. "Smooth" growth takes place when layer-to-layer growth occurs. In case of true layer-by-layer growth, the growth front as shown in Fig. 7 should show no overlap between successive layers n. It is obvious that the larger the overlap, the rougher the growth front is, and that eventually at extreme cases a three-dimensional front will be observed. As one can see, at a given V/III flux ratio and gallium flux, the growth front is better at higher temperatures where surface mirgration is high. Surface atoms move then rapidly to kink sites and edge steps and growth takes place by a layer-by-layer mechanism. The accompanying increased evaporation rate of Ga at high temperatures does not in this case play an important role since migration is the dominant mechanism. In other words, the high surface migration occurring at elevated temperatures improves the quality of the growth front.

Figures 8(a) and 8(b) show the contour and three-dimensional (3D) plot of the growth front at 400 °C; Figs. 9(a) and 9(b) show similar plots at 500 °C. The legend on the side in each figure indicates the number of monolayers of the growth front. As one sees, the growth front is 3 monolayers (ML) at 500 °C, and 4 ML at 400 °C. This clearly suggests that the growth front is improved as the temperature is increased; however, as the temperature increases, the growth rate decreases rapidly. Furthermore, as the temperature goes beyond a certain point, entropy-controlled effects will cause a poor quality of film due to high defect densities. From this point of view one can say that there is a temperature "window" in which a good growth front can be obtained with reasonably high growth rates.

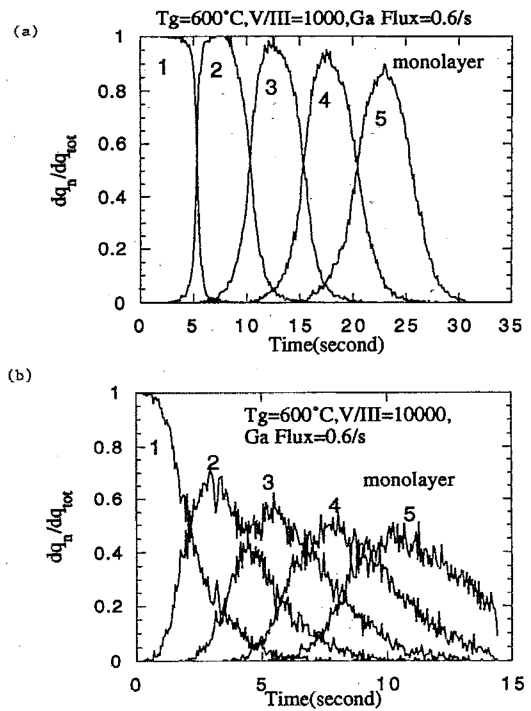

FIG. 10. (a) Ratio of nth layer coverage over total coverage vs growth temperature (T=600 °C, V/III=1000, Ga flux=0.61/s); (b) ratio of nth layer coverage over total coverage vs growth temperature (T=600 °C, V/III =10 000, Ga flux=0.61/s).

C. Impact of V/III flux ratio on the growth front

For the study of the impact of V/III flux ratio on the growth front, the growth temperature was kept constant, and Ga flux was kept at 0.6/s. The dq_n/dq_{tot} plots are shown in Figs. 10(a) (V/III=1000) and 10(b) (V/III=10 000). The contours and 3D plots are shown in Figs. 11(a) and 11(b), respectively, for V/III=1000; Figs. 12(a) and 12(b) give similar plots for V/III=10 000.

As one sees, the growth front becomes rougher at high V/III ratios. The growth front of the V/III=1000 case corresponds to 3 ML, a situation which is close to a layer-by-layer growth mechanism. When the V/III ratio increases to, say, 10 000, the growth front corresponds to 6 ML. The growth rate is about 2 s/ML for the V/III=10 000 case, and becomes 5 s/ML for the V/III=1000 case. Low V/III ratio corresponds to the good growth front; however, if the V/III ratio is too low, the growth rate becomes too low for practical applications.

The larger growth rate at high V/III ratios can be understood by the model described in Sec. II. One could see in that section that an increase of group-V atoms increases the probability of nitrogen to meet gallium atoms and be trapped by them. The degradation of growth front at high V/III ratios can be explained as follows. As we have seen, the increasing of V/III ratio results in increased incorporation of gallium and nitrogen. In this condition, the growth may happen at free sites, which leads to forming island structures. As a result, the growth becomes 3D and the growth front become rougher.

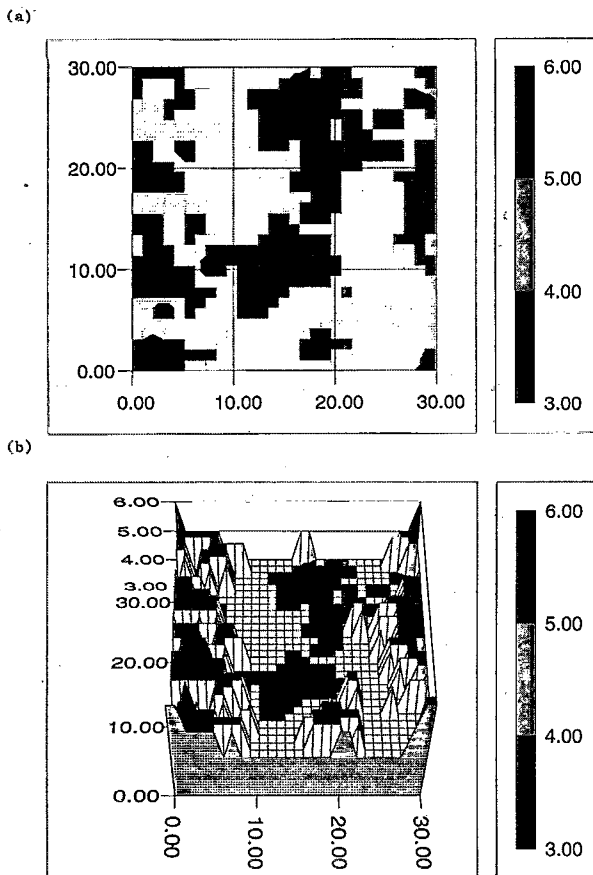

FIG. 11. (a) Growth front contour (T=600 °C, V/III=1000); the legend of the right-hand side is the number of surface monolayers; (b) 3D plot of growth front (T=600 °C, V/III=1000); the legend on the right-hand side is the number of surface monolayers.

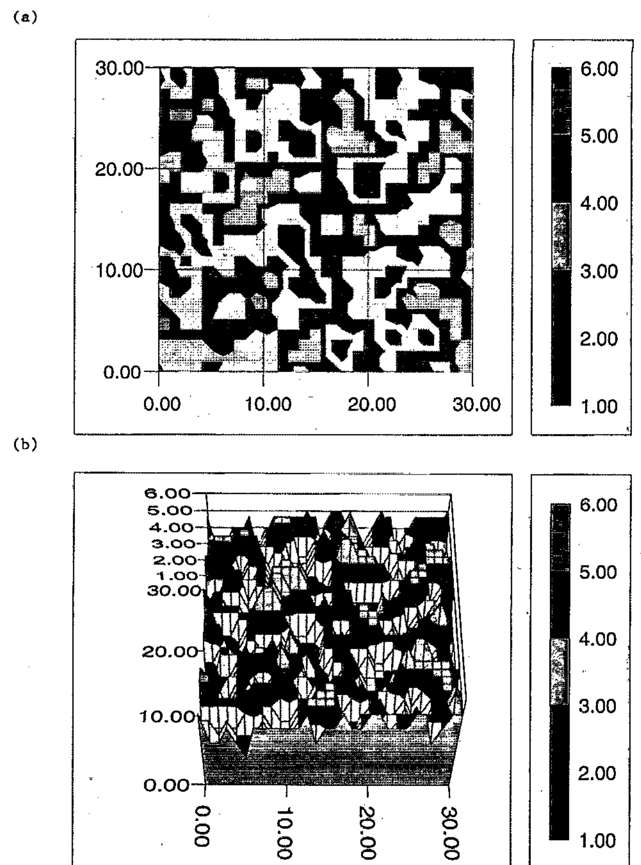

FIG. 12. (a) Growth front contour (T=600 °C, V/III=10 000); the legend on the right-hand side is the number of surface monolayers; (b) 3D plot of growth front (T=600 °C, V/III=10 000); the legend on the right-hand side is the number of surface monolayers.

D. Impact of Ga and N flux on the growth rate and the roughness of the growth front

Simulations of the dependence of growth rate on Ga flux were made at a constant temperature of 600 °C. The results are given in Fig. 13 which shows that the growth rate is dependent on the Ga flux. As the Ga flux increases the growth rate increases; however, as the Ga flux increases, the growth front becomes rougher. From Figs. 14(a) and 14(b) the growth front takes 4 ML at a Ga flux of 0.6161/s, but takes 6 ML at a Ga flux of 3.08 atoms/s. This indicates that as the gallium incorporation increases, 3D growth starts taking place as explained earlier on in Sec. III C.

The impact of N flux was finally discussed in Sec. III C where the role of the V/III ratio was examined. The results indicate that for given Ga flux, the higher the N flux is, the rougher the growth front.

IV. CONCLUSIONS

Monte Carlo approaches have been used to simulate the growth process of GaN. The growth rate and the quality of the growth front are determined by the substrate temperature, Ga flux, and V/III ratio. At a given temperature and V/III ratio, the lower the Ga flux, the better the growth front. At a given temperature, the lower the V/III ratio, the better the growth front, but the lower the growth rate. There is a temperature window in which a good growth front can be obtained with reasonably high growth rates. Improvement of the quality of growth front may be obtained by using external sources (other than substrate temperature) such as light and ions to enhance the Ga surface kinetics. As-grown GaN may be associated with a cation stabilized surface. This could account for the high intrinsic carrier concentration of-

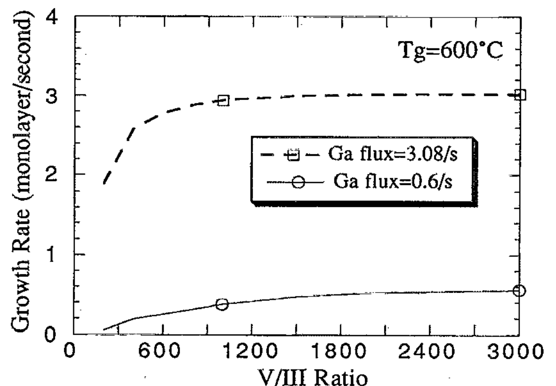

FIG. 13. Growth rate vs Ga flux and V/III ratio.

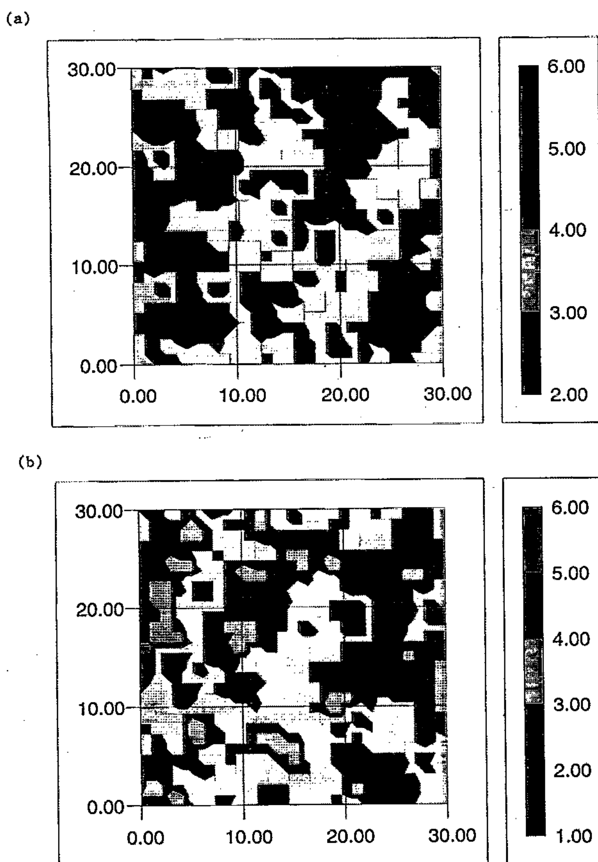

FIG. 14. (a) Growth front contour (T=400 °C, Ga flux=0.61/s); the legend on the right-hand side is the number of surface monolayers; (b) growth front contour (T=600 °C, Ga flux=3.08/s); the legend on the right-hand side is the number of surface monolayers.

ten observed in this material. Nitrogen incorporation occurs preferably at the kink sites (sites near step edges). Sample orientation and surface preparation would play an important role in the incorporation of nitrogen in the growth of GaN. Experimental verification of the suggested Ga-stabilized surface conditions would shed the light on the growth mechanisms of GaN.

ACKNOWLEDGMENTS

The authors would like to thank Dr. Max Yoder of ONR for his support and Dr. Chang-Hee Hong, Kyushik Hong, and Marcel Tutt for helpful discussions. Work supported by ONR Contract No. N00014-92-J1552.

[1] H. P. Maruska and J. J. Tietjen, Appl. Phys. Lett. **15**, 327 (1969).
[2] S. Strite and H. Morkoç, J. Vac. Sci. Technol. B **10**, 1237 (1992).
[3] R. F. Davis, Proc. IEEE **79**, 702 (1991).
[4] D. Elwell and M. M. Elwell, Prog. Cryst. Growth Charact. **17**, 53 (1988).
[5] M. J. Paisley and R. F. Davis, J. Cryst. Growth **127**, 136 (1993).
[6] J. I. Pankove, Mater. Res. Soc. Symp. Proc. **162**, 515 (1990).
[7] C. D. Thurmond, J. Electrochem. Soc. **119**, 622 (1972).
[8] R. C. Powell, N. E. Lee, Y. W. Kim, and J. E. Greene, J. Appl. Phys. **73**, 189 (1993).
[9] J. Singh, Rev. Solid State Sci. **4**, 785 (1990).
[10] C. R. Eddy, Jr. and T. D. Moustakas, J. Appl. Phys. **73**, 448 (1993).
[11] R. C. Powell, Appl. Phys. Lett. **60**, 2505 (1992).
[12] B. J. Min, C. T. Chan, and K. M. Ho, Phys. Rev. B **45**, 1159 (1992).
[13] H. Okumura, S. Misawa, and S. Yoshida, Appl. Phys. Lett. **59**, 1058 (1991).
[14] M. J. Paisley, Z. Sitar, L. B. Posthill, and R. F. Davis, J. Vac. Sci. Technol. A **7**, 701 (1989).
[15] R. C. Powell, G. A. Tomasch, Y. W. Kim, J. A. Thornton, and J. E. Green, Mater. Res. Soc. Symp. Proc. **162**, 525 (1990).
[16] T. Lei, M. Fancinlli, R. J. Molnar, T. D. Moustakas, R. J. Graham, and J. Seanlon, Appl. Phys. Lett. **59**, 944 (1991).
[17] J. Singh and J. Arias, J. Vac. Sci. Technol. A **7**, 2562 (1989).
[18] J. R. Arthur, Surf. Sci. **43**, 1999 (1974).
[19] C. T. Foxon and B. A. Joyce, Surf. Sci. **64**, 293 (1977).
[20] J. Singh and K. K. Bajaj, J. Vac. Sci. Technol. B **2**, 576 (1984).
[21] R. T. Sanderson, *Chemical Bonds and Bond Energy* (Academic, New York, 1976).
[22] J. Karpinski, J. Cryst. Growth **66**, 1 (1984).
[23] S. Nagata and T. Tanaka, J. Appl. Phys. **48**, 950 (1977).
[24] J. H. Neave, P. J. Dobson, B. A. Joyce, and J. Zheng, Appl. Phys. Lett. **47**, 100 (1985).
[25] S. Strite, J. Ruan, Z. Li, A. Salvador, H. Chen, David J. Smith, W. J. Choyke, H. Morkoç, J. Vac. Sci. Technol. B **9**, 1924 (1991).